Inorg. Chem. **2002**, *41*, 6161–6168

Syntheses and Characterizations of Copper(II) Polymeric Complexes Constructed from 1,2,4,5-Benzenetetracarboxylic Acid

Rong Cao,*,† Qian Shi,†,‡ Daofeng Sun,† Maochun Hong,† Wenghua Bi,† and Yingjun Zhao†

State Key Laboratory of Structural Chemistry, Fujian Institute of Research on the Structure of Matter, The Chinese Academy of Sciences, Fuzhou, 350002, P.R. China, and Department of Chemistry, Wenzhou Teachers College, Wenzhou, 325000, P.R. China

Received July 8, 2002

Four polymeric complexes with rectangular grids or channels, $[Cu_2(btec)(H_2O)_4 \cdot 2H_2O]_n$ (**2**), $[Cu_2(btec)_{4/4}\{Cu(Hbtec)_{2/2}(4,4'\text{-Hbpy})(H_2O)_2\}_2 \cdot 4H_2O]_n$ (**3**), $[Cu_2(btec)(hmt)(H_2O)_4 \cdot 8H_2O]_n$ (**4**), and $[Cu_3(btec)(OH)_2]_n$ (**5**), were designed and constructed from Cu(II) ion and 1,2,4,5-benzenetetracarboxylic acid along with auxiliary ligands (where H_4btec = 1,2,4,5-benzenetetracarboxylic acid, 4,4′-Hbpy = monoprotonated 4,4′-bipyridine, and hmt = hexamethylenetetramine). Complexes **2**, **3**, and **4** have rectangular pores with the size of 6.5 Å × 4.5 Å, 6 Å × 7 Å, and 10.1 Å × 11.8 Å, respectively, while **5** has a channel of 7.4 Å × 9.6 Å. The complexes show interesting magnetic properties due to the different coordination modes of the carboxylate groups and the presence of auxiliary ligands. On lowering the temperature, the magnetic interactions in **2** are changed from antiferromagnetic to ferromagnetic. For **3**, the antiferromagnetic interactions weaken sharply at low temperature. Complex **4** shows ferromagnetic interactions while **5** is antiferromagnetic.

Introduction

The design of metal−organic materials with large channels and cavities has been deeply researched, due to their intriguing structural diversity and potential functions as microporous solids for molecular adsorption, ion exchange, and heterogeneous catalysis.[1−3] In particular, multibenzenecarboxylate ligands have been shown to be good building blocks in the design of metal−organic materials with desired topologies owing to their rich coordination modes. In spite of the rich coordination chemistry exhibited by 1,4-benzenedicarboxylic and 1,3,5-benzenetricarboxylic acids, studies on 1,2,4,5-benzenetetracarboxylic acid (H_4btec) are less reported, presumably because, for steric reasons, all of the four carboxyl groups are unlikely to engage in coordination to metal ions. However, through carefully controlling the reaction conditions, we have found that H_4btec is also a versatile building block for the construction of metal−organic complexes through complete or partial deprotonation of its carboxyl groups, and a series of interesting structures have been successfully obtained.[4,5] With the aim of understanding the coordination chemistry of H_4btec, we recently began studies on the assembly reactions of H_4btec with metal ions via solution or hydrothermal synthetic methods.[6] In particular, we were interested in such reactions in the presence of auxiliary ligands, and we have successfully synthesized two

* Author to whom correspondence should be addressed. E-mail: rcao@ms.fjirsm.ac.cn.

† The Chinese Academy of Sciences.

‡ Wenzhou Teachers College.

(1) (a) Hagrman, P. J.; Hagrman, D.; Zubieta, J. *Angew. Chem., Int. Ed.* **1999**, *38*, 2639. (b) Batten, S. R.; Robson, R. *Angew. Chem., Int. Ed.* **1998**, *37*, 1460. (c) Yaghi, O. M.; Li, H.; Davis, C.; Richardson, D.; Groy, T. L. *Acc. Chem. Res.* **1998**, *31*, 474.

(2) (a) Sato, O.; Iyoda, T.; Fujishima, A.; Hashimoto, K. *Science* **1996**, *271*, 49. (b) Evans, O. R.; Xiong, R.; Wang, Z.; Wong, G.. K.; Lin, W. *Angew. Chem., Int. Ed.* **1999**, *38*, 536. (c) Fujita, M.; Kwon, Y. J.; Washizu, S.; Ogura, K. *J. Am. Chem. Soc.* **1994**, *116*, 1151.

(3) (a) Eddaoudi, M.; Kim, Jaheon; Rosi, N.; Vodak, David; Wachter, J.; O'Keeffe, M.; Yaghi, O. M. *Science* **2002**, *295*, 469. (b) Harrison, R. G.; Fox, O. D.; Meng, M. O.; Dalley, N. K.; Barbour, L. J. *Inorg. Chem.* **2002**, *41*, 838.

(4) (a) Usubaliev, B. T.; Shnulin, A. N.; Mamedov, Kh. S. *Koord. Khim.* **1982**, *8*, 1532. (b) Robl, C. *Z. Anorg. Allg. Chem.* **1987**, *554*, 79. (c) Robl, C.; Hentschel, S. *Mater. Res. Bull.* **1991**, *26*, 1355. (d) Cheng, D.-P.; Zheng, Y.-Q.; Lin, J.-L.; Xu, D.-J.; Xu, Y.-Zh. *Acta Crystallogr., Sect. C* **2000**, *56*, 523.

(5) (a) Chu, D.-Q.; Xu, J.-Q.; Duan, L.-M.; Wang, T.-G.; Tang, Ao.-Q.; Ye, L. *Eur. J. Inorg. Chem.* **2001**, *5*, 1135. (b) Rochon, F. D.; Massarweh, G. *Inorg. Chim. Acta* **2000**, *304*, 190. (c) Wu, Ch.-D.; Lu, C.-Zh.; Lu, Sh.-F.; Zhuang, H.-H.; Huang, J.-Sh. *Inorg. Chem. Commun.* **2002**, *5*, 171. (d) Gutschke, S. O. H.; Price, D. J.; Powell, A. K.; Wood, P. T. *Eur. J. Chem.* **2001**, 2739. (e) Murugavel, R.; Krishnamurthy, D.; Sathiyendiran, M. *J. Chem. Soc., Dalton Trans.* **2002**, 34.

(6) (a) Shi, Q.; Cao, R.; Sun, D.-F.; Hong, M.-Ch.; Liang, Y.-C. *Polyhedron* **2001**, *20*, 3287. (b) Cao, R.; Sun, D.-F.; Liang, Y.-C.; Hong, M.-Ch.; Tatsumi, K.; Shi, Q. *Inorg. Chem.* **2002**, *41*, 2087. (c) Sun, D.-F.; Cao, R.; Liang, Y.-C.; Shi, Q.; Hong, M.-Ch. *J. Chem. Soc., Dalton Trans.* **2002**, *8*, 1847.

10.1021/ic0258577 CCC: $22.00
Published on Web 10/23/2002

Table 1. Crystallographic Data for Complexes **2**−**5**

	2	**3**	**4**	**5**
chem formula	$C_{10}H_{14}Cu_2O_{14}$	$C_{50}H_{42}Cu_4N_4O_{32}$	$C_{16}H_{38}Cu_2N_4O_{20}$	$C_{10}H_8Cu_3O_{10}$
fw	485.30	1465.04	733.58	957.56
T, K	293(2)	293(2)	293(2)	293(2)
color	green	dark green	blue-green	green
size	0.12 × 0.18 × 0.22	0.10 × 0.15 × 0.18	0.15 × 0.18 × 0.20	0.12 × 0.16 × 0.20
cryst syst	triclinic	triclinic	monoclinic	triclinic
space group	$P\bar{1}$	$P\bar{1}$	*C*2/*c*	$P\bar{1}$
a, Å	6.5156(6)	7.8533(6)	14.7908(4)	5.0155(1)
b, Å	6.9194(6)	9.8667(8)	13.9157(3)	5.8109(12)
c, Å	9.3157(9)	17.8567(14)	15.5121(4)	9.6258(19)
α, deg	95.319(2)	102.002(1)		98.85(3)
β, deg	108.664(2)	93.833(2)	114.987(1)	92.06(3)
γ, deg	108.164(2)	105.407(1)		94.27(3)
V, Å^3	369.33(6)	1293.78(18)	2893.94(12)	276.11(10)
Z	0.5	1	4	0.5
D_{calc}, Mg·m^{-3}	1.091	1.880	1.684	1.440
μ, mm^{-1}	1.481	1.734	1.561	2.895
R^a	0.0643	0.0567	0.0578	0.0213
$R_w{}^b$	0.1755	0.1609	0.1664	0.0599

[a] $R = \sum(|F_o| - |F_c|)/\sum F_o|$. [b] $R_w = \{\sum w[(F_o^2 - F_c^2)^2]/\sum w[(F_o^2)^2]\}^{1/2}$. $w = 1/[\sigma^2(F_o^2) + (aP)^2 + bP]$, where $P = (F_o^2 + 2F_c^2)/3$.

novel polymeric complexes from H_4btec and 1,10-phenathroline in our previous work.[6a] This prompted us to extend our work by using other auxiliary ligands, especially those bridging ligands such as 4,4′-bipyridine, pyrazine, etc. Considering the special bioactive and biocatalytic functions of the copper(II) carboxylate complexes[7] along with their interesting magnetic properties, we focused our work on the Cu(II) and H_4btec system. Herein we will report four interesting polymeric complexes, $[Cu_2(btec)(H_2O)_4{\cdot}2H_2O]_n$ (**2**), $[Cu_2(btec)_{4/4}\{Cu(Hbtec)_{2/2}(4,4'\text{-Hbpy})(H_2O)_2\}_2{\cdot}4H_2O]_n$ (**3**), $[Cu_2(btec)(hmt)(H_2O)_4{\cdot}8H_2O]_n$ (**4**), and $[Cu_3(btec)(OH)_2]_n$ (**5**), obtained from the assembly reactions of the Cu(II) ion and H_4btec in the presence of auxiliary ligands of pyrazine, 4,4′-bipyridine (4,4′-bpy), hexamethylenetetramine (hmt), and imidazole.

Experimental Section

Elemental analyses of carbon, hydrogen, and nitrogen were carried out on an Elementar Vario ELIII. The infrared spectroscopy on KBr pellets was performed on a Nicolet Magna FT-IR 750 spectrometer in the range 200−4000 cm^{-1}. Electronic reflectance spectra were recorded on a Lambda 35 spectrometer. Variable-temperature magnetic susceptibilities were determined in the temperature range 4−300 K on a Quantum Design MPMS SQUID magnetometer at 10 T. Corrections were applied for diamagnetism calculated from Pascal constants. Effective magnetic moments were calculated by the equation $\mu_{eff} = 2.828(\chi_M T)^{1/2}$, where χ_M is the magnetic susceptibility per formula unit. All reagents were commercially available and used as received.

$[Cu_2(btec)(H_2O)_4{\cdot}2H_2O]_n$ (2). A solution of $CuCl_2{\cdot}2H_2O$ (0.17 g, 1.0 mmol) in 10 cm^3 of H_2O was slowly added to a water solution (30 cm^3) of H_4btec (0.12 g, 0.5 mmol), and the mixture was heated to boiling for 15 min. A MeOH solution of pyrazine (0.08 g, 1.0 mmol) was added dropwise into the above solution, and the solution was adjusted to pH = 4 by the addition of 10% NaOH solution. The mixture was filtered and evaporated at room temperature for 1 week to give green crystals of **2** (81 mg, yield 48% based on $CuCl_2{\cdot}2H_2O$). Anal. Calcd for $C_{10}H_{14}Cu_2O_{14}$: C, 24.74; H, 2.89. Found: C, 24.85; H, 2.82.

$[Cu_2(btec)_{4/4}\{Cu(Hbtec)_{2/2}(4,4'\text{-Hbpy})(H_2O)_2\}_2{\cdot}4H_2O]_n$ (3). This complex was prepared similarly to **2** with the exception that pyrazine was replaced by 4,4′-bipy and the pH value was adjusted to 2. Dark-green crystals of **3** were obtained after standing at room temperature for 3 weeks (88 mg, yield 52% based on $CuCl_2{\cdot}2H_2O$). Anal. Calcd for $C_{50}H_{42}Cu_4N_4O_{32}$: C, 40.95; H, 2.87; N, 3.83. Found: C, 40.49; H, 2.83; N, 3.95.

$[Cu_2(btec)(hmt)(H_2O)_4{\cdot}8H_2O]_n$ (4). This complex was prepared similarly to **2** with the replacement of pyrazine by hmt, and blue-green crystals of **4** were formed after standing at room temperature for 1 day (139 mg, yield 82% based on $CuCl_2{\cdot}2H_2O$). Anal. Calcd for $C_{16}H_{38}Cu_2N_4O_{20}$: C, 26.19; H, 5.18; N, 7.64. Found: C, 26.12; H, 5.15; N, 7.72.

$[Cu_3(btec)(OH)_2]_n$ (5). $CuCl_2{\cdot}2H_2O$ (0.08 g, 0.5 mmol), H_4btec (0.12 g, 0.5 mmol), imH (0.04 g, 0.5 mmol), and NaOH (0.04 g, 1 mmol) were added to a 1:1 (v/v) MeOH−H_2O solution (20 cm^3) in a Teflon-lined stainless steel reactor. The mixture was heated at 140 °C for 2 days, and green blocklike crystals were formed after the mixture cooled to room temperature (70 mg, yield 87% based on $CuCl_2{\cdot}2H_2O$). Anal. Calcd for $C_{10}H_4Cu_3O_{10}$: C, 25.29; H, 0.84. Found: C, 25.25; H, 0.90.

X-ray Crystallography. X-ray intensities of the four complexes were collected on a Siemens Smart CCD diffractometer with graphite-monochromated Mo Kα radiation (λ = 0.71073 Å) with the ω scan mode. Empirical absorption corrections were applied to the data using the SADABS program.[8] The structures were solved by direct methods.[9] Non-hydrogen atoms were refined anisotropically. Hydrogen atoms in **2** were generated in idealized positions. In **3** and **4**, the hydrogen atoms for the C and N atoms were generated from successive difference Fourier syntheses. One pyridyl ring of 4,4′-bipy in **3** was handled disordered in two positions. In **5**, all hydrogen atoms were generated in idealized positions, except that for the hydroxide group was generated from difference Fourier synthesis. All calculations were performed using the SHELXTL program.[10] The crystallographic data and other pertinent information are summarized in Table 1.

(7) (a) King, R. B. *Encyclopedia of Inorganic Chemistry*; Wiley: New York, 1994. (b) Mathrubootham, V.; Rathinam, V.; Mallayan, P. *Inorg. Chem.* **1998**, *37*, 6418.
(8) Sheldrick, G. M. *SADABS, Program for Empirical Absorption Correction of Area Detector Data*; University of Göttingen: Göttingen, 1996.
(9) Sheldrick, G. M. *SHELXS 97, Program for Crystal Structure Solution*; University of Göttingen: Göttingen, 1997.
(10) Sheldrick, G. M. *SHELXL 97, Program for Crystal Structure Refinement*; University of Göttingen: Göttingen, 1997

Table 2. Characteristic IR Absorption Bands for the Title Complexes (cm^{-1})

	ν_{as}(COO)	ν_s(COO)	$\Delta\nu$	ν (COOH)	ν_{M-N}	ν_{M-O}	ν_{N-H}	ν_{H_2O}	ν_{OH}
Na_4btec	1515(s)	1420(s)	95						
complex **2**	1576(s)	1375(s)	201			305(m)		3525(s)	
	1492(s)	1420(s)	72						
complex **3**	1581(s)	1365(s)	216	1739(s)	436(m)	356(m)	3510(s)	3446(s)	
	1491(s)	1417(s)	74						
complex **4**	1560(s)	1370(s)	190		430(m)	315(m)		3480(s)	
complex **5**	1601(s)	1389(s)	212			362(m)			3515(s)

Chart 1

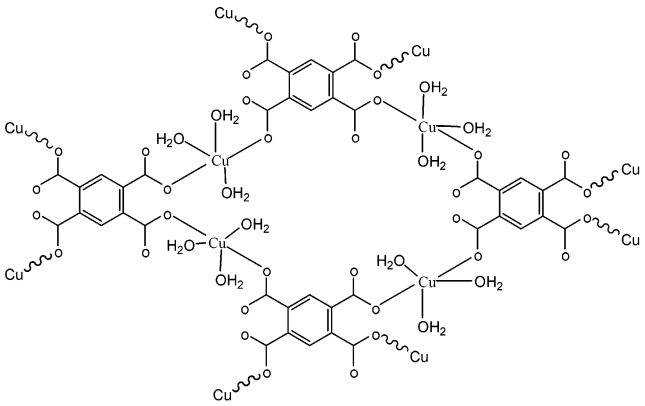

Results and Discussion

Synthesis and General Characterization. The self-assembly reaction of Cu(II) and H_4btec in solution gave rise to a layer structure of $[Cu_2(btec)(H_2O)_6\cdot 4H_2O]_n$[4a] (**1**) as shown in Chart 1. If some of the coordinated water molecules on Cu(II) in **1** are replaced by bridging ligands, such as pyrazine and 4,4′-bipyridine (4,4′-bpy), 2-D and 3-D open-frameworks with variable cavities and channels may be reasonably expected. Taking account of the deprotonation process, $H_4btec \leftrightarrow H_3btec^- + H^+ \leftrightarrow H_2btec^{2-} + 2H^+ \leftrightarrow Hbtec^{3-} + 3H^+ \leftrightarrow btec^{4-} + 4H^+$, in the formation of the products, we sense that a low pH value may lower the deprotonation rate of H_4btec and thereby the formation of the products, which may be helpful for the crystal growth. Thus in our synthetic reactions, the pH value was adjusted to lower than 7. Interestingly, the results we got are somewhat out of our expectation. In the presence of pyrazine, the reaction of H_4btec and Cu(II) yielded an unexpected complex $[Cu_2(btec)(H_2O)_4\cdot 2H_2O]_n$ (**2**), in which pyrazine is not present. If the reaction was carried out without pyrazine, the isolation of **2** failed and **1** was obtained. Thus pyrazine may act as template to direct the formation of **2** although the detailed mechanism still remains unclear. If 4,4′-bpy was used to replace pyrazine, the reaction generated another interesting complex, $[Cu_2(btec)_{4/4}\{Cu(Hbtec)_{2/2}(4,4'\text{-Hbpy})(H_2O)_2\}_2\cdot 4H_2O]_n$ (**3**), which is constructed from the paddle-wheel $[Cu_2(OOCR)_4]$ building units in the layer and constrained by Cu−btec−Cu−L (L = 4,4′-Hbpy) chains beside the layer. When hmt was introduced into the reaction system, $[Cu_2(btec)(hmt)(H_2O)_4\cdot 8H_2O]_n$ (**4**) was produced, where the coordination mode of $btec^{4-}$ is the same as that in **1**, and one of the coordinated water molecules in **1** is replaced by μ_2-hmt to form the three-dimensional framework of **4**.

We also introduced solvothermal methods into our synthetic reactions and hoped to obtain complexes with high dimensions and unexpected structures. Unfortunately, the ligands mentioned above (pyrazine, 4,4′-bpy, and hmt) produced redox reactions with Cu(II) at high temperature, and only unknown mixtures were obtained. When another stable ligand, imH, was used in the reaction, a new complex, $[Cu_3(btec)(OH)_2]_n$ (**5**), was formed in high yield, and the attempt to synthesize **5** without imH failed. This result indicates that imH plays an important role in the formation of **5**, probably through acting as a reaction template and deprotonation reagent.

The main absorption peaks in the IR spectra of the four complexes are listed in Table 2. The difference in ν_{as}(COO) and ν_s(COO) ($\Delta\nu$), compared to the corresponding values in sodium carboxylate (95 cm^{-1} in Na_4btec), is currently employed to determine the corresponding mode of the carboxylate group. In complex **2**, the values of $\Delta\nu$ show that the carboxylate groups coordinate to the Cu(II) atoms both in monodentate (201 cm^{-1} > 95 cm^{-1})[11,12] and in bidentate (72 cm^{-1} < 95 cm^{-1})[12,13] fashions. In **3**, besides the two coordination fashions as in **2** ($\Delta\nu$ = 216 and 74 cm^{-1}), an uncoordinated protonated carboxylate group is present with the characteristic absorption at 1739 cm^{-1}. The absorption at 3510 cm^{-1} is assigned to ν_{N-H} of the protonated N atom in 4,4′-Hbpy. As for **4** and **5**, the values of $\Delta\nu$ (190 and 212 cm^{-1} respectively) indicate that the carboxylate groups coordinate to the Cu(II) atoms only as monodentate ligands. The coordination modes of carboxylate groups in the four complexes are summarized in Chart 2.

Descriptions of the Crystal Structures. The selected bond lengths and angles of complexes **2**−**5** are listed in Tables 3 and 4.

$[Cu_2(btec)(H_2O)_4\cdot 2H_2O]_n$ (2). All carboxylic groups of the organic ligand in **2** are deprotonated, in agreement with the IR spectrum, where no absorption peak around 1730 cm^{-1} for a protonated carboxylic group is observed. Each of two *p*-carboxylate groups of $btec^{4-}$adopts a bidentate bridging coordination mode, while each of the other two adopts a monodentate coordination mode, and the whole ligand acts as μ_6-bridge linking six Cu(II) ions (Chart 2c). As shown in the ORTEP drawing of **2** (Figure 1a), two bridging carboxylate groups from two $btec^{4-}$ bridge two Cu(II) ions to form a binuclear unit that can be viewed as the basic building block of the structure. The square-pyramidal arrangement of the Cu(II) atom is completed by two carboxyl O atoms from two $btec^{4-}$ ligands and two water O atoms in the equatorial plane (average deviation: 0.0319 Å), and one

(11) Nakamoto, K. *Infrared and Raman Spectra of Inorganic and Coordination Compounds*, 3rd ed.; Wiley: New York, 1978.
(12) (a) Wang, Y.-Y.; Shi, Q.; Shi, Q.-Zh. Gao, Y.-C.; Zhou, Zh.-Y. *Polyhedron* **1999**, *18*, 2009. (b) Shi, Q.; Cao, R.; Hong, M.-Ch. *Transition Met. Chem*. **2001**, *26*, 657.
(13) Brzyska, W.; Kowalewicz, J. *Zesz. Nauk. Politech. Slask., Chem*. **1981**, *677*, 141.

Chart 2

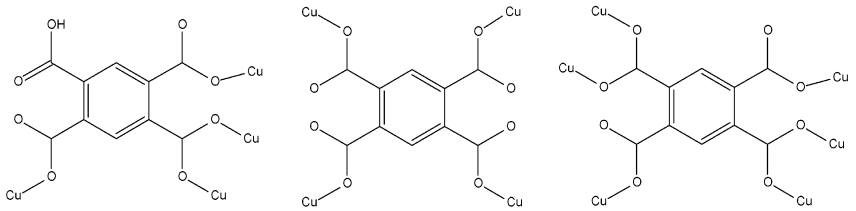

Table 3. Selected Bond Lengths (Å) for Complexes **2**,[a] **3**,[b] **4**,[c] and **5**[d]

	Complex **2**		
Cu−O(3A)	1.955(4)	Cu−O(1)	1.957(4)
Cu−O(6)	1.973(4)	Cu−O(5)	1.977(5)
Cu−O(4B)	2.245(4)		
	Complex **3**		
Cu(1)−O(5A)	1.946(5)	Cu(1)−O(1)	1.953(5)
Cu(1)−O(14)	1.991(5)	Cu(1)−N(1)	2.037(7)
Cu(1)−O(13)	2.266(8)	Cu(2)−O(8)	1.951(5)
Cu(2)−O(7B)	1.958(5)	Cu(2)−O(11C)	1.972(4)
Cu(2)−O(12D)	1.981(4)	Cu(2)−O(9)	2.160(4)
Cu(2)−Cu(2B)	2.6926(16)		
	Complex **4**		
Cu−O(1A)	1.942(3)	Cu−O(3)	1.974(3)
Cu−O(6)	1.993(4)	Cu−N(1)	2.084(4)
Cu−O(5)	2.202(4)		
	Complex **5**		
Cu(1)−O(5A)	1.9473(15)	Cu(1)−O(5)	1.9473(15)
Cu(1)−O(3)	1.9900(16)	Cu(1)−O(3A)	1.9900(16)
Cu(2)−O(4)	1.9373(16)	Cu(2)−O(1B)	1.9512(16)
Cu(2)−O(5C)	1.9565(16)	Cu(2)−O(5D)	1.9783(16)
Cu(2)−Cu(2E)	2.9510(11)		

[a] Key: (A) $-x, -y+1, -z$; (B) $x, y-1, z$. [b] Key: (A) $x-1, y-1, z$; (B) $-x+2, -y, -z$; (C) $-x+3, -y, -z$; (D) $x-1, y, z$. [c] Key: (A) $-x+{}^1/_2, y+{}^1/_2, -z+{}^1/_2$. [d] Key: (A) $-x, -y+1, -z$; (B) $x, y-1, z$; (C) $-x-1, -y+1, -z$; (D) $x-1, y-1, z$; (E) $-x-2, -y, -z$.

Table 4. Selected Bond Angles (deg) for Complexes **2**,[a] **3**,[b] **4**,[c] and **5**[d]

	Complex **2**		
O(3A)−Cu−O(1)	93.87(18)	O(3A)−Cu−O(6)	166.11(19)
O(1)−Cu−O(6)	89.12(18)	O(3A)−Cu−O(5)	92.92(19)
O(1)−Cu−O(5)	167.6(2)	O(6)−Cu−O(5)	81.89(19)
O(3A)−Cu−O(4B)	102.81(16)	O(1)−Cu−O(4B)	87.95(16)
O(6)−Cu−O(4B)	90.84(16)	O(5)−Cu−O(4B)	100.6(2)
	Complex **3**		
O(5A)−Cu(1)−O(1)	170.7(3)	O(5A)−Cu(1)−O(14)	89.9(2)
O(1)−Cu(1)−O(14)	87.5(2)	O(5A)−Cu(1)−N(1)	87.3(2)
O(1)−Cu(1)−N(1)	93.5(2)	O(14)−Cu(1)−N(1)	169.3(3)
O(5A)−Cu(1)−O(13)	99.9(3)	O(1)−Cu(1)−O(13)	89.2(3)
O(14)−Cu(1)−O(13)	96.5(3)	N(1)−Cu(1)−O(13)	94.2(3)
O(8)−Cu(2)−O(7B)	167.0(2)	O(8)−Cu(2)−O(11C)	89.3(2)
O(7B)−Cu(2)−O(11C)	89.1(2)	O(8)−Cu(2)−O(12D)	88.8(2)
O(7B)−Cu(2)−O(12D)	89.8(2)	O(11C)−Cu(2)−O(12D)	166.83(18)
O(8)−Cu(2)−O(9)	108.26(19)	O(7B)−Cu(2)−O(9)	84.75(19)
O(11C)−Cu(2)−O(9)	100.41(18)	O(12D)−Cu(2)−O(9)	92.56(18)
	Complex **4**		
O(1A)−Cu−O(3)	167.39(16)	O(1A)−Cu−O(6)	90.57(16)
O(3)−Cu−O(6)	88.36(16)	O(1A)−Cu−N(1)	86.66(15)
O(3)−Cu−N(1)	93.18(15)	O(6)−Cu−N(1)	173.97(19)
O(1A)−Cu−O(5)	96.18(17)	O(3)−Cu−O(5)	96.42(15)
O(6)−Cu−O(5)	92.8(2)	N(1)−Cu−O(5)	92.82(17)
	Complex **5**		
O(5A)−Cu(1)−O(5)	180.00(9)	O(5A)−Cu(1)−O(3)	89.76(7)
O(5)−Cu(1)−O(3)	90.24(7)	O(5A)−Cu(1)−O(3A)	90.24(7)
O(5)−Cu(1)−O(3A)	89.76(7)	O(3)−Cu(1)−O(3A)	180.00(9)
O(4)−Cu(2)−O(1B)	95.57(7)	O(4)−Cu(2)−O(5C)	89.54(7)
O(1B)−Cu(2)−O(5C)	170.60(6)	O(4)−Cu(2)−O(5D)	155.58(6)
O(1B)−Cu(2)−O(5D)	95.48(7)	O(5C)−Cu(2)−O(5D)	82.83(7)
Cu(1)−O(5)−Cu(2C)	113.54(7)	Cu(1)−O(5)−Cu(2F)	111.85(7)
Cu(2C)−O(5)−Cu(2F)	97.17(7)		

[a] Key: (A) $-x, -y+1, -z$; (B) $x, y-1, z$. [b] Key: (A) $x-1, y-1, z$; (B) $-x+2, -y, -z$; (C) $-x+3, -y, -z$; (D) $x-1, y, z$. [c] Key: (A) $-x+{}^1/_2, y+{}^1/_2, -z+{}^1/_2$. [d] Key: (A) $-x, -y+1, -z$; (B) $x, y-1, z$; (C) $-x-1, -y+1, -z$; (D) $x-1, y-1, z$; (F) $x+1, y+1, z$.

carboxyl O atom from the third $btec^{4-}$ ligands in the axial position. The binuclear Cu(II) units are linked by the monodentate carboxylate groups in $btec^{4-}$, producing a stepped-like 2D structure with grids of 6.5 Å × 4.5 Å as shown in Figure 1b. Numerous hydrogen-bonding interactions are present between O(water)···O(carboxyl) and O(carboxyl)···O(carboxyl), forming a 3D channel-like network (Figure 1c).

$[Cu_2(btec)_{4/4}\{Cu(Hbtec)_{2/2}(4,4'\text{-Hbpy})(H_2O)_2\}_2\cdot 4H_2O]_n$ (3). The crystal structure analysis reveals that **3** is a neutral 2D polymer. Tetranuclear species $[Cu_2(btec)_{4/4}\{Cu(Hbtec)_{2/2}(4,4'\text{-Hbpy})(H_2O)_2\}_2]$ constitute the basic building block, which is composed of one Cu_2 paddle-wheel secondary building unit (SBU) and two mononuclear Cu(II) motifs (Figure 2a). The paddle-wheel SBU is completed by four carboxylate groups, two from $btec^{4-}$ and two from $Hbtec^{3-}$, with the Cu−Cu distance being 2.6926(16) Å. Two coordination modes for benzenetetracarboxylate ligands are present: (a) All carboxyl groups are deprotonated ($btec^{4-}$); two para ones take part in the organization of two SBUs in bidentate bridging mode, while the remaining two link the other two SBUs at axial positions in a monodentate mode (Chart 2c). Hence, each $btec^{4-}$ ligand connects four SBUs, forming an infinite 2D layer with rectangular pores (6 Å × 7 Å), and two guest water molecules per pore are present. (b) Only three carboxyl groups are deprotonated ($Hbtec^{3-}$) and take part in the coordination; the protonated one remains free (Chart 1a). The carboxylate group para to the protonated carboxyl group is used to complete the paddle-wheel SBU in bidentate bridging mode. The other two carboxylate groups link two mononuclear copper motifs in monodentate mode, and each such motif attaches to two $Hbtec^{3-}$, generating 1D chains that can be viewed as paralleled Cu−Hbpy barriers on the two sides of the SBU layer (Figure 2b). Cu(1) in mononuclear motif is surrounded by two water O atoms, two carboxylate O atoms, and one N atom from monoprotonated 4,4′-Hbpy, giving an O_4N distorted square-based pyramidal conformation. The protons of 4,4′-Hbpy were generated from successive difference Fourier syntheses in solving the structure and confirmed by the IR spectrum. The presence of terminally coordinating Hbpy is unprecedented, and previous reports show that coordinating 4,4′-Hbpy is usually observed in main group metal systems.[14−16]

(14) Chen, Ch.-Y.; Lo, F.-R.; Kao, H.-M.; Lii, K.-H. *Chem. Commun.* **2000**, 1061.
(15) Chen, Ch.-Y.; Chun, P. P.; Lii, K.-H. *Chem. Commun.* **1999**, 1473.
(16) Wirth, A.; Lange, I.; Henschel, D.; Moers, O.; Biaschetter, A.; Jones, P. G. *Z. Anorg. Allg. Chem.* **1998**, *624*, 1308.

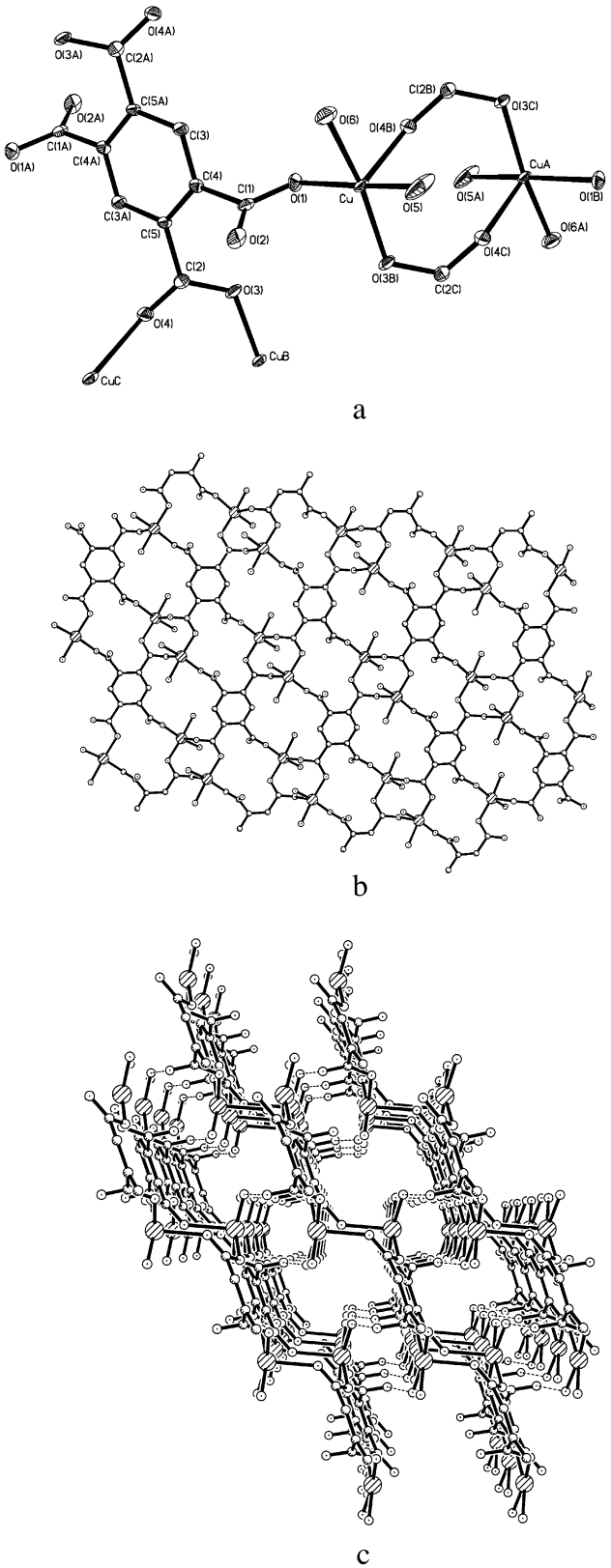

Figure 1. (a) ORTEP drawing of **2**, drawn with displacement ellipsoids at the 50% probability level. (b) The 2D porous structure in **2** along the *a* axis. (c) Packing structure along the *c* axis of **2**.

$[Cu_2(btec)(hmt)(H_2O)_4 \cdot 8H_2O]_n$ (4). The structure of **4** is formed by replacing one O atom of the coordinated water molecule on the Cu(II) ion in **1**[4a] by an N atom from a μ_2-hmt ligand to give rise to a three-dimensional framework.

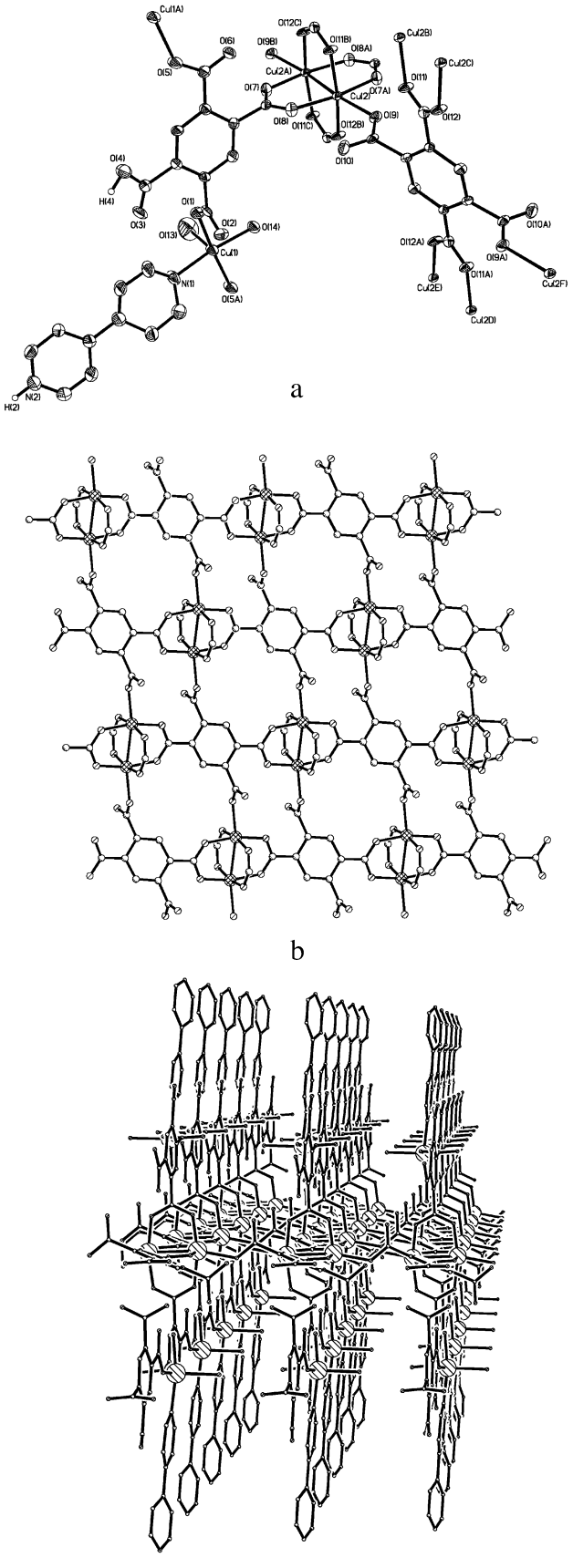

Figure 2. (a) ORTEP view of **3**, drawn with displacement ellipsoids at the 50% probability level. (b) View of the layer structure formed by Cu_2 SBUs in **3**. The copper motifs outside the layer are omitted for clarity. (c) Packing structure along the *a* axis for **3**.

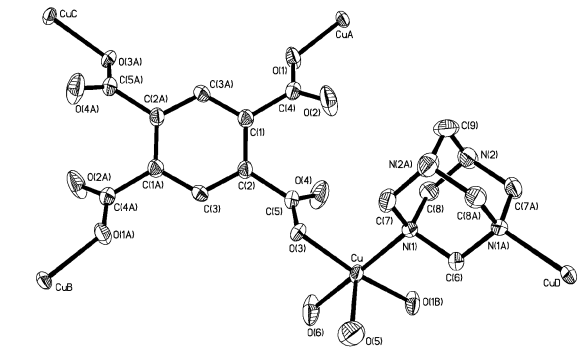

a

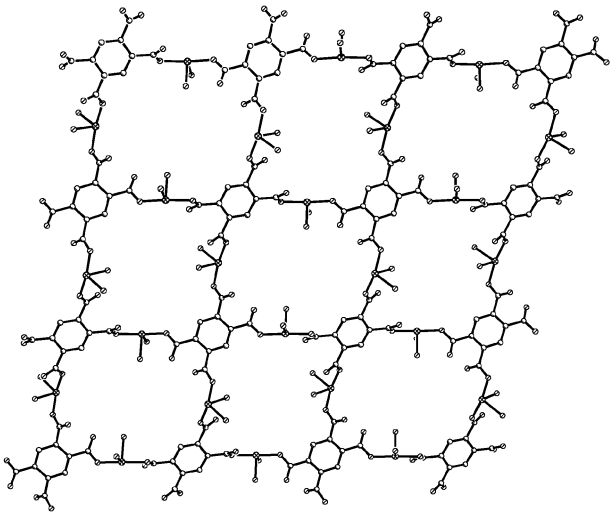

b

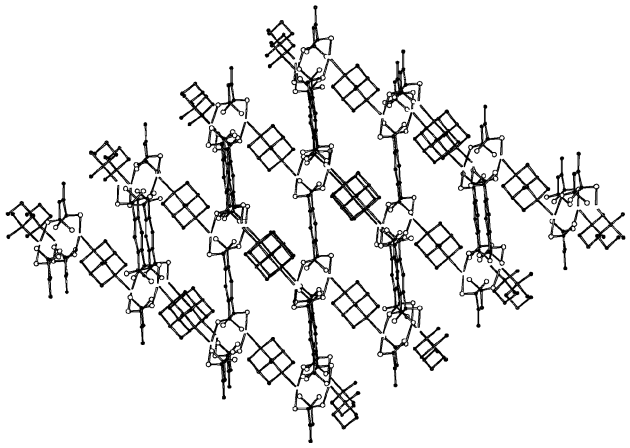

c

Figure 3. (a) ORTEP view of **4**, drawn with displacement ellipsoids at the 50% probability level. (b) View of the grid structure along the *c* axis in **4**. (c) Packing structure along the *b* axis for **4**.

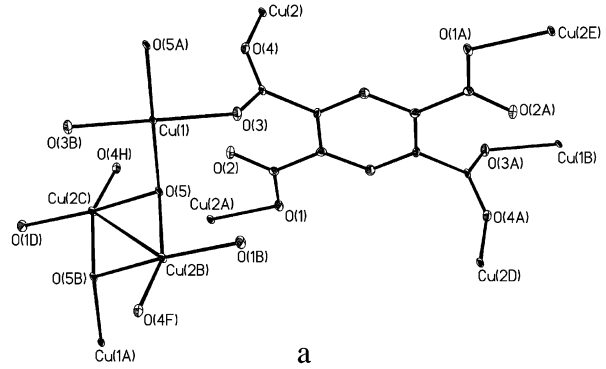

a

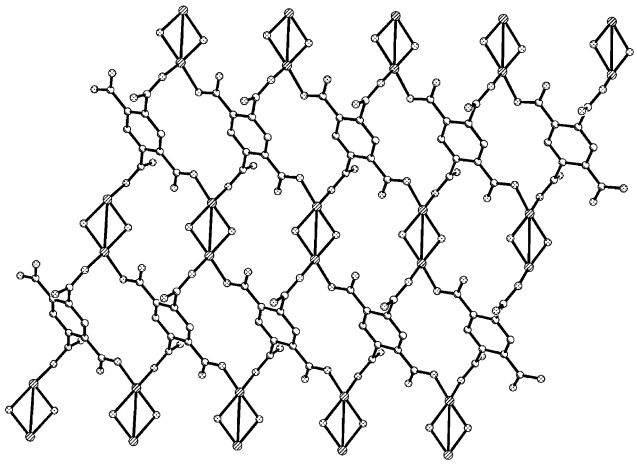

b

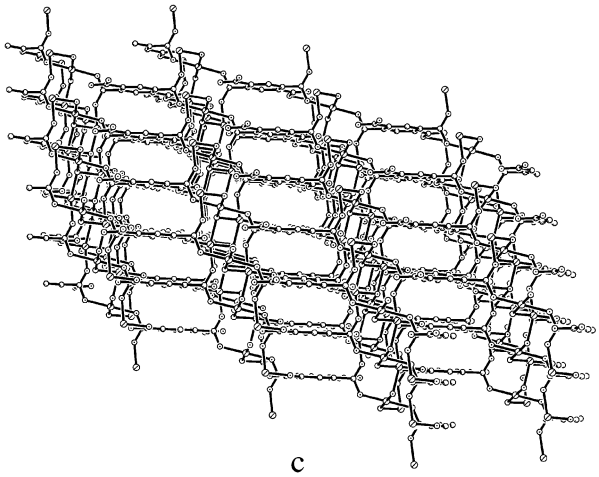

c

Figure 4. (a) ORTEP view of **5**, drawn with displacement ellipsoids at the 50% probability level. (b) View of the rectangular grid wall of the metal hydroxide members in **5**. The phenyl rings in $btec^{4-}$ were omitted for clarity. (c) Packing structure with channels along the *b* axis for **5**.

The local coordination environment around the Cu(II) ion is shown in Figure 4a. All carboxylic groups of 1,2,4,5-benzenetetracarboxylic acid are deprotonated, and each of them adopts a monodentate coordination mode (Chart 2b). Each hmt ligand acts as a μ_2-bridge linking two Cu(II) ions through its two nitrogen atoms. The Cu(II) ion is surrounded by two carboxylate O atoms, one water O atom and one hmt N atom in the equatorial plane, and one water O atom at the axial position, forming a square-based pyramidal arrangement (Figure 3a). If we neglect hmt ligands, a layer structure similar to that in **1**[4a] is observed in **4**: each $btec^{4-}$ ligand links four Cu(II) ions and each Cu(II) ion attaches to two $btec^{4-}$ ligands to form the 2D layer, which consists of 4 + 4 grids with the size of 10.1 Å × 11.8 Å; the phenyl rings stand at the corners while the Cu(II) atoms stand in the sides of the grids (Figure 3b). Through Cu−N bonding, the hmt ligands further link the layers into a 3D network with

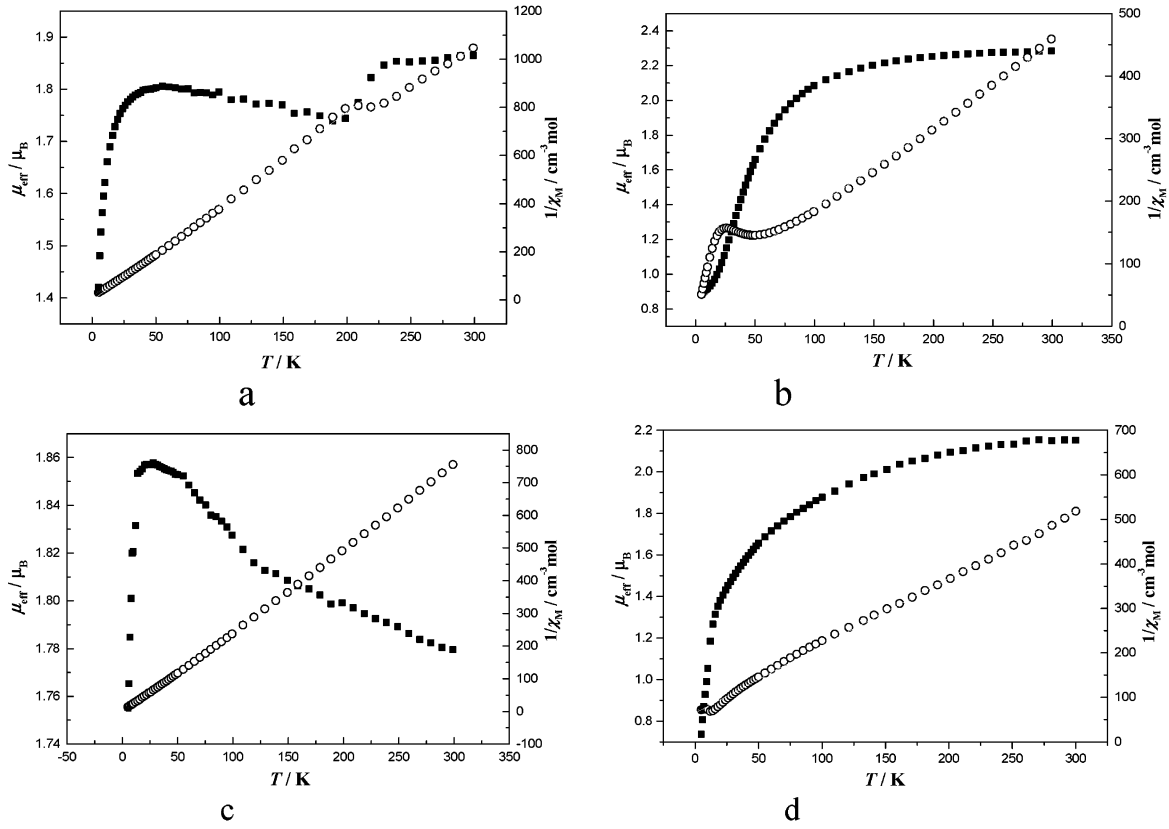

Figure 5. The effective magnetic moment μ_{eff} versus T plots for the complexes: (a) **2**, (b) **3**, (c) **4**, and (d) **5**.

rhombic channels filled by guest water molecules (Figure 3c). Numerous hydrogen-bonding interactions [O(carboxyl)···O(water) (2.796(5), 2.596(6), 2.770(5), 2.725(8), 2.794(19), and 2.750(9) Å) and O(water)···O(water) (2.64(3) Å)] exist in the structure.

$[Cu_3(btec)(OH)_2]_n$ (5). The local coordination environment around metal ions in **5** is given in Figure 4a. The coordination mode of the carboxylate groups in $btec^{4-}$ is similar to that in **2**, two of which adopt a monodentate mode, and the other two adopt a bidentate-bridging mode (Chart 2c). The hydroxide group acts as μ_3-bridge linking three Cu(II) ions. There are two kinds of Cu(II) ions in the structure: one (Cu(1)) is coordinated by two hydroxide oxygen atoms and two oxygen atoms from bridging carboxylate groups in an exactly square planar geometry; the other is coordinated by two hydroxide oxygen atoms, one oxygen from a monodentate carboxylate group, and one oxygen from a bridging carboxylate group in a slightly distorted square planar geometry (Figure 4a). Dinuclear species formed by two Cu(2) and two OH^- with an interatomic distance of 2.951(1) Å may be viewed as the subunit for the structure of **5**. Each Cu_2 unit attaches to four oxygen atoms from four $btec^{4-}$, among which two come from monodentate and the other two from bidentate carboxylate groups. Thus each Cu_2 unit links four $btec^{4-}$ ligands to form a two-dimensional porous layer structure (Figure 4b). The layers are further connected by Cu(1) links through Cu−O bonding from the remaining oxygen atoms of bridging carboxylate and OH^- groups, completing the μ_3-bridging mode of hydroxide and yielding the final three-dimensional structure with channels of 7.4 Å × 9.6 Å along the *b* axis (Figure 4c).

Table 5. Structure Comparison of Complexes **2**−**5**

	bond distances (Å)		
complex	Cu−O/N(equatorial)$_{av}$	Cu−O(axial)	Cu···Cu
2	1.9655	2.245(4)	5.985
3			
Cu(1)	1.9818	2.266(8)	7.545
Cu(2)	1.9655	2.160(4)	2.6922
4	1.9982	2.202(4)	5.922(htm)
			8.173(btec)
5			
Cu(1)	1.9687		2.951
Cu(2)	1.9558		3.252
			3.266

Comparison of the Structures. The coordination conformations of the Cu(II) atoms are all square-planar pyramidal except in **5**. The bond lengths around the Cu(II) ion in the five complexes are summarized in Table 5. All Cu−O and Cu−N bond lengths in the equatorial plane **2**−**4** and for **5** show typical values for Cu(II) ion. In the axial position, the Cu−O bond lengths increase in the sequence **3**(Cu(2) < **4** < **2** < **3**(Cu(1).

The Cu(II)···Cu(II) distance in the binuclear unit of **2** (5.985 Å) is much longer than the corresponding value 2.6922 Å in **3**, due to the different bond directions of the bridging carboxylate groups. In **2**, two carboxylate O atoms coordinate to the Cu(II) atom in equatorial and axial positions, resulting in the long Cu(II)···Cu(II) distance, while, in the paddle-wheel SBU of **3**, each bridging carboxylate group and the two Cu(II) ions are almost coplanar to yield the short Cu(II)···Cu(II) distance. The Cu(II)···Cu(II) distance through the bridge of two *p*-carboxylate groups in **3** is 7.545 Å, shorter than the value 8.173 Å through the bridge of two *o*-carboxylate groups in **4**, but longer than that through

Table 6. Electronic Reflectance Data for **2**−**5**

	$\tilde{\nu}/10^3$ cm^{-1}		
complex	band I	band II	band III
2	13.4, 10.8	24.8	40.2
3	14.4, 9.8	28.7	40.0, 42.6
4	12.9, 10.0	25.4, 27.6	32.2, 40.8
5	14.9	26.3	30.3

the hmt bridge in **4** (5.922 Å). The distances between two Cu(II) centers bridged by hydroxyl groups in **5** are 2.951 Å for Cu(2)···Cu(2), 3.252 and 3.266 Å for Cu(1)···Cu(2), shorter than the corresponding values in **2**, **3**, and **4**, except that in the Cu_2 paddle-wheel secondary building unit for **3**. Most of the μ_3-hydroxo bridged Cu(II) complexes reported are tetranuclear,[17−20] and the separations between two Cu(II) atoms and angles of Cu−O−Cu are similar to that in **5**. The different coordination direction along with different Cu(II)···Cu(II) distances influence the magnetic properties of the complexes as discussed below.

Electronic Spectra. The reflectance spectra of the complexes in the solid state were recorded in the 200−1100 nm range, and the data are listed in Table 6. The intense reflectance bands (band III) at higher frequencies are assigned to the intraligand transitions in the complexes. The absorptions at band II are assigned to the carboxylate-to-copper charge-transfer band (LMCT). The visible reflectance spectra also contain bands at 13.4 with a shoulder 10.8×10^3 cm^{-1} for **2**, 14.4 with a shoulder 9.8×10^3 cm^{-1} for **3**, and 12.9 with a shoulder 10.0×10^3 cm^{-1} for **4**, characteristic of a copper(II) $d_{xz},d_{yz} \rightarrow d_{x^2-y^2}(^2B_1 \rightarrow {}^2E)$[21] transition in a tetragonal ligand field, in which the copper(II) atom has a distorted square-based pyramidal coordination environment. The absorption at 14.9×10^3 cm^{-1} without a shoulder for **5** is assigned to copper(II) $d_{xz},d_{yz} \rightarrow d_{x^2-y^2}(^2B_{1g} \rightarrow {}^2E_g)$[22] transitions in a square-planar ligand field. The information obtained from the electronic spectra about the coordination configurations of the copper(II) ions in the complexes is in agreement with those found from the structural data.

Magnetic Properties. The plots of the effective magnetic moment μ_{eff} versus T for complexes **2**−**5** are shown in Figure 5. For **2**, as shown in Figure 5a, the μ_{eff} value at room temperature, 1.86 μ_B, is slightly higher than the spin-only value for Cu^{II} (1.73 μ_B), decreases smoothly from 300 to 229 K, and decreases sharply to reach 1.74 μ_B at 188 K. On further lowering the temperature, the value increases gradually to 55 K and decreases abruptly to reach the minimum value of 1.42 μ_B at 5 K. The data fit the Curie−Weiss law with the parameters of $\Theta = -31.2$ K in the temperature range 300−188 K and $\Theta = 0.466$ K from 188 K to 5 K, indicating that the interactions between two Cu(II) centers through the effective exchange media of carboxylate group are antiferromagnetic at normal atmospheric temperature, and change to weak ferromagnetic on lowering the temperature with $T_N = 188$ K.

The effective magnetic moment for **3** decreases from 2.28 μ_B at 300 K to 0.88 μ_B at 5 K, suggesting the existence of antiferromagnetic interactions among the Cu(II) atoms, mainly due to the presence of paddle-wheel unit $[Cu_2(O_2CR)_4L_2]$. It is interesting that the coupling interactions weaken at the low temperature, with the Weiss constant $\Theta = -44.9$ K at the temperature range of 300−26 K, and $\Theta = -0.135$ K below 26 K as shown in Figure 5b.

The effective magnetic moment μ_{eff} versus T plot for **4** is shown in Figure 5c. The μ_{eff} value is 1.78 μ_B at 300 K, which is slightly higher than 1.73, increases gradually to 1.86 μ_B at 24 K, and then sharply decreases to 1.76 μ_B at 5 K, implying the presence of ferromagnetic interactions between Cu(II) atoms. The Weiss constant is $\Theta = 2.32$ K. The ferromagnetic coupling may exchange through both carboxylate bridges and hmt ligands.

For **5**, the effective magnetic moment for 1.5 Cu(II) atoms per mole decreases from 2.15 μ_B at 300 K to 0.74 μ_B at 5 K (Figure 5d), and $\Theta = -42.7$ K from the Curie−Weiss fitting, suggesting the existence of strong antiferromagnetic interactions between the Cu(II) atoms. In the complex, both the carboxylate group and the hydroxo group might act as the effective supercoupling exchange media.

Conclusion

Four polymeric copper(II) complexes with rectangular grids or channels, $[Cu_2(btec)(H_2O)_4 \cdot 2H_2O]_n$ (**2**), $[Cu_2(btec)_{4/4}\{Cu(Hbtec)_{2/2}(4,4'\text{-Hbpy})(H_2O)_2\}_2 \cdot 4H_2O]_n$ (**3**), $[Cu_2(btec)(hmt)(H_2O)_4 \cdot 8H_2O]_n$ (**4**), and $[Cu_3(btec)(OH)_2]_n$ (**5**), were constructed from 1,2,4,5-benzenetetracarboxylic acid in the presence of auxiliary ligands. The auxiliary ligands play an important role in the syntheses of the complexes through engaging in coordination or acting as templates. The coordination modes of the carboxylate groups in the four complexes are different, and the difference is confirmed by IR spectra. The configuration of the Cu(II) atoms is square-based pyramidal in **2**−**4** and square-planar in **5**. The UV−vis reflectance spectra are consistent with the crystal structures. The magnetic properties of the complexes are interesting. The exchange interactions in **2** and **3** are changed on lowering the temperature, especially for **2**. Complex **4** shows ferromagnetic interactions while **5** is antiferromagnetic. The different magnetic behaviors of the complexes may come from the different coordination modes of carboxylate ligands and the existence of auxiliary ligands.

Acknowledgment. The authors thank the NNSFC, Natural Science Foundation of Fujian Province, and the key project of CAS for financial support.

Supporting Information Available: X-ray crystallographic files in CIF format for four crystalline forms **2**−**5**, the hydrogen bond distances existing in the four complexes, and a figure of the reflectance spectra of the complexes in the solid state. This material is available free of charge via the Internet at http://pubs.acs.org.

IC0258577

(17) Dedert, P. L.; Sorrell, T.; Marks, T. J.; Ibers, J. A. *Inorg. Chem.* **1982**, *21*, 3506.
(18) Sakamoto, M.; Itose, S.; Ishimori, T.; Matsumoto, N.; Okawo, H.; Kida, S. *J. Chem. Soc., Dalton Trans.* **1989**, 2083.
(19) Sletten, J.; Sørensen, A.; Julve, M.; Journaux, Y. *Inorg. Chem.* **1990**, *29*, 5054.
(20) Chen, L.-Q.; Thompson, L. K.; Bridson, J. N. *Inorg. Chem.* **1993**, *32*, 2938.
(21) Melnik, M. *Coord. Chem. Rev.* **1981**, *36*, 287.
(22) Araya, L.; Vargas, J.; Costamagna, J. *Transition Met. Chem.* **1986**, *11*, 321.